IJCSI International Journal of Computer Science Issues, Vol. 8, Issue 5, No 3, September 2011
ISSN (Online): 1694-0814
www.IJCSI.org

Fault Location in Transmission System Using Phasor Measurement Unit

Satyabrata Das[1], Soumya Ranjan Mohanty[2] and Sabyasachi Pattnaik[3]

[1]Asstt Prof., Department of CSE, College of Engineering Bhubaneswar Orissa, India-751024

[2]Asstt Prof., Department of EE, Motilal Neheru National Institute of Technology Allahabad, India-211004

[3]Prof., Department of I&CT, Fakir Mohan University Balasore, India -756019

Abstract

The concept of Synchrophasor and Global positioning system Phasor measurement unit placed in the transmission system plays a vital role for correct localization of the fault. In this context the PMU based fault location is addressed in this paper for correct decision of the distance relay. So as a whole the problem of the protection scheme for transmission system is viewed as a problem of signal processing rather than instrumentation. Further with the concept of Synchrophasor and Phasor measurement unit the fault location in a transmission system can be achieved without the knowledge of transmission line parameter.

Keywords: *synchrophasors; GPS; Phasor Measurement Units (PMU); DFR.*

1. Introduction

As the electric power grid continues to expand and as transmission lines are pushed to their operating limits, the dynamic operation of the power system has become more of a concern and has become more difficult to accurately model. In addition, the ability to affect real-time system control is developing into a need in order to prevent wide scale cascading outages. For decades, control centres have estimated the "state" of the power system (the positive sequence voltage and angle at each network node) from measurements of the power flows through the power grid. It is very desirable to be able to "measure" the system state directly and/or augment existing estimators with additional information.

For over 100 years, phasors were used for analyzing AC quantities assuming a constant frequency in the power system. A relatively new variant of this technique that synchronizes the calculation of a phasor to absolute time has been developed, which is known as synchronized phasor measurement or synchrophasors.

The development of communications and the introduction and availability of a standardized time reference over wide geographic areas by Global Positioning System(GPS), laid the foundation for the Synchrophasor technology. This in turn has provided the information for system-wide monitoring and control of the power system that was not previously available.

In this paper, we have presented an analysis of fault detection and fault location based on the use of synchrophasors. Current and voltage phasors at both ends of a transmission line are measured by Phasor Measurement Units (PMU) and are sent to a central location using communication link and are synchronously compared to determine the state of the system at that particular instant.

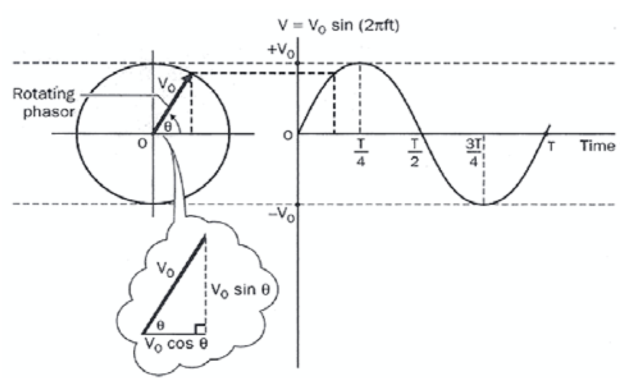

Fig. 1 Phasors and Synchrophasors

Accurate fault location reduces operating costs by avoiding lengthy and expensive patrols. It also expedites repairs and restoration of lines, ultimately reducing revenue loss caused by outages. The provided analysis effectively detects and locates any fault with a fair amount of precision.

Phasors are basic tools of AC circuit analysis, usually introduced as a means of representing steady state sinusoidal wave forms of fundamental power frequency. Even when a power system is not quite in a steady state, phasors are often useful in describing the behaviour of the power system. Synchrophasors are phasors synchronized with an absolute (common) time reference by means of global positioning system (GPS). By synchronizing two phasors which maybe hundreds of kms apart they can be put on same phasor diagram.

2. GPS – An overview

The Global Positioning Satellite (GPS) system consists of 24 satellites in six orbits at an approximate altitude of 10,000 miles above the surface of the earth. The GPS system consists of space segment, ground segment and users. The ground segment consists of 6 radio stations which control and monitor position and time. The user segment is responsible for the calculation of coordinates of the receiver and time based on the interpreted messages from the satellites.

The satellites transmit a one-pulse per-second coded signal, along with an identifier for the signal that can be interpreted by the earth station receivers Time synchronization accuracy of 0.2μ sec can be achieved[2,1].

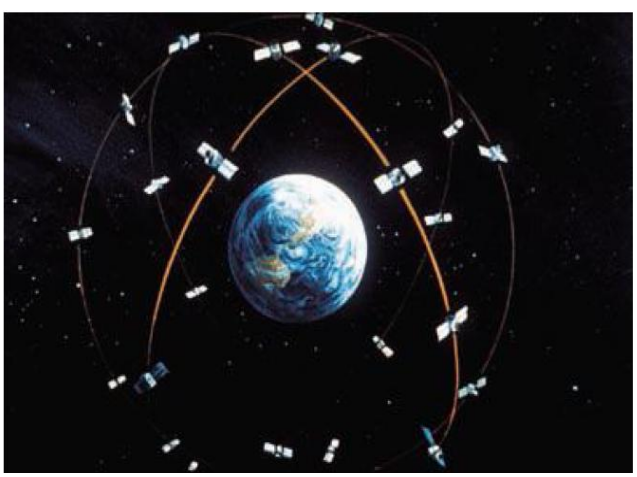

Fig. 2 Global Positioning Satellite (GPS)

2.1 Phasor Measurement Unit (PMU)

Phasor measurement units (PMUs) are power system devices that provide synchronized measurements of real-time phasors of voltages and currents. Synchronization is achieved by same-time sampling of voltage and current waveforms using timing signals from the Global Positioning System Satellite (GPS). Synchronized phasor measurements elevate the standards of power system monitoring, control, and protection to a new level. They are located in substations

The GPS receiver provides the 1 pulse-per-second (pps) signal, and a time tag, which consists of the year, day, hour, minute, and second. The time could be the local time, or the UTC (Universal Time Coordinated).

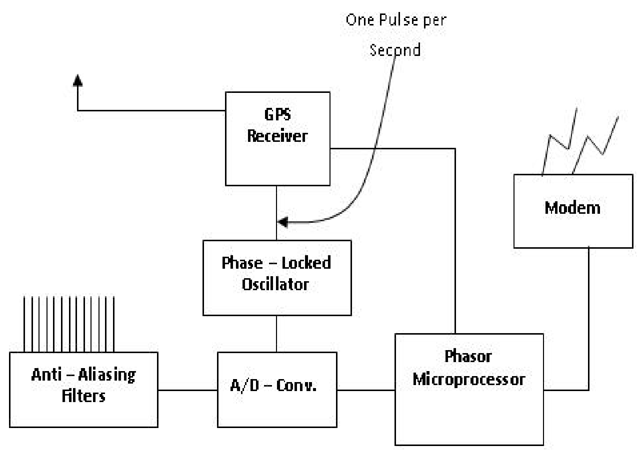

Fig. 3 Basic PMU Structure

2.1.1 Basic PMU Structure

The l-pps signal is usually divided by a phase-locked oscillator into the required number of pulses per second for sampling of the analog signals. In most systems being used at present, this is 12 times per cycle of the fundamental frequency. The analog signals are derived from the voltage and current transformer secondaries, with appropriate anti-aliasing and surge filtering. The microprocessor determines the positive sequence phasors according to the recursive algorithm described previously, and the timing message from the GPS, along with the sample number at the beginning of a window, is assigned to the phasor as its identifying tag. The computed string of phasors, one for each of the positive sequence measurements, is assembled in a message stream to be communicated to a remote site. The messages are transmitted over a dedicated communication line[4,3].

Benefits of PMUs

It provides precise measurement of the power system state that can be obtained at frequent intervals, enabling dynamic phenomena to be observed from a central location, and appropriate control actions can be taken.

Post-disturbance analysis is much improved because precise snapshots of the system states are obtained through GPS synchronization.

Advanced protection based upon synchronized phasor measurements is possible

2.1 Phasor Data Concentrator (PDC)

Phasor data concentrator (PDC) gathers data from several PMUs; it rejects bad data, aligns the time stamps, and creates a coherent record of simultaneously recorded data from wider part of power system. The data is stored at this stage for analysis and post mortem. The data is transferred to the super Phasor Data Concentrator (PDC) via special communication link as per the protocol defined by IEEE standards C37.1 18. Any protection and control envisaged for the particular area is implemented at this level in real time[5]. Time latency is present but manageable. At a higher level, the super data concentrator does similar function as part of PDC for entire system. The super concentrator is usually at the main controlling centre called Energy Management Centre (EMC).

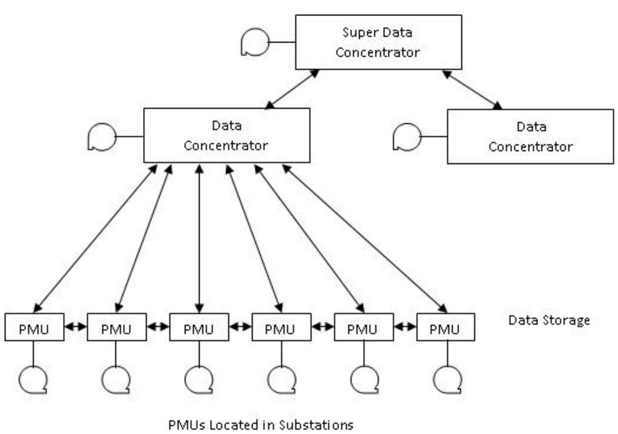

Fig. 4 PMUs Located in substation

2.2.1 Working of PMU using GPS:

Following is a brief description of present sampling and signal processing practices for synchronized phasor measurement, oscillography, harmonic analysis, and line distance protection.

Fixed time interval sampling

Traditionally, digital fault recorders (DFRs) acquire data at fixed time intervals to provide voltage and current oscillography and harmonic analysis. For example, DFRs use sampling rates of 1 kilo samples/second or faster. The samples are synchronized to an internal time source or an external time source. In some applications, the external time source is an absolute time reference from a global positioning system (GPS) receiver[5].

Figure 5 shows a typical DFR data acquisition block diagram with traditional DFR applications (such as oscillography and harmonic analysis) using an internal time source. The system includes a hardware low-pass filter (Hardware LPF) for anti-aliasing and an analog-to-digital (A/D) converter for analog-to-digital conversion.

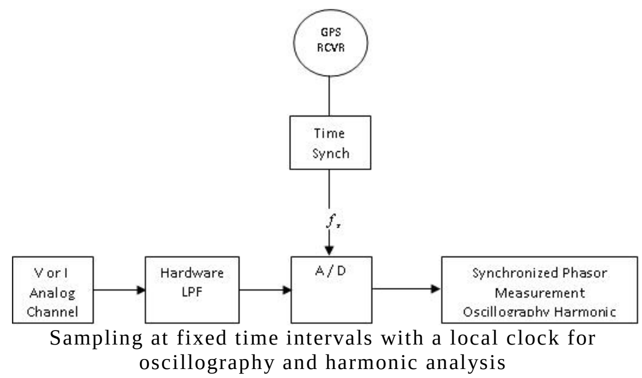

Fig. 5 DFR data acquisition block diagram

The main advantage of this acquisition system is that the data preserve the frequency information of the power system. This data acquisition system is also suitable for synchronized phasor measurement when an external time source with absolute time reference determines the sampling interval.

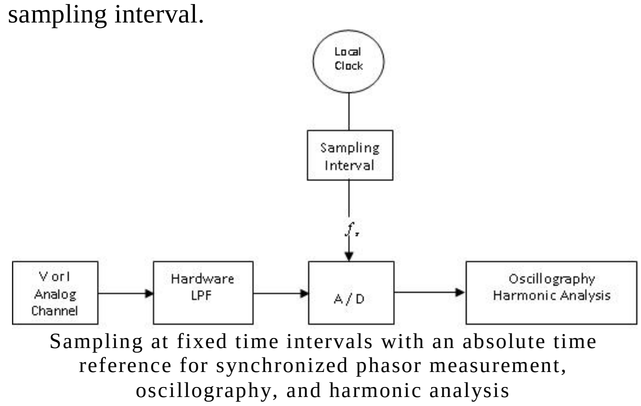

Fig. 6 DFR data acquisition block diagram with fixed sampling rate

3. Simulation Results

3.1 Model with Parameters

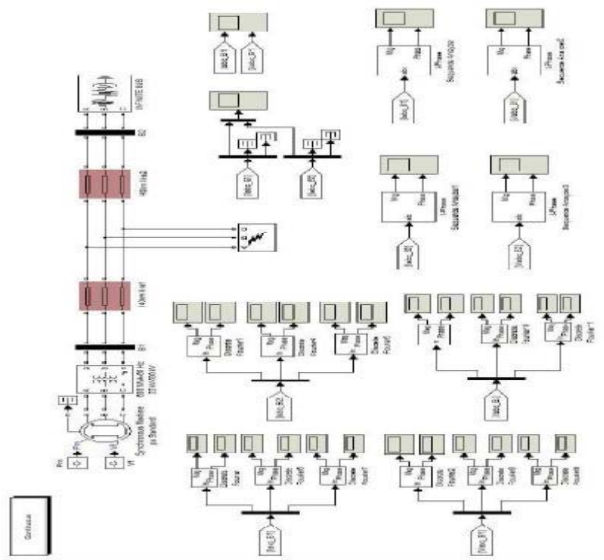

Fig. 7 Transmission Line Model With Fault

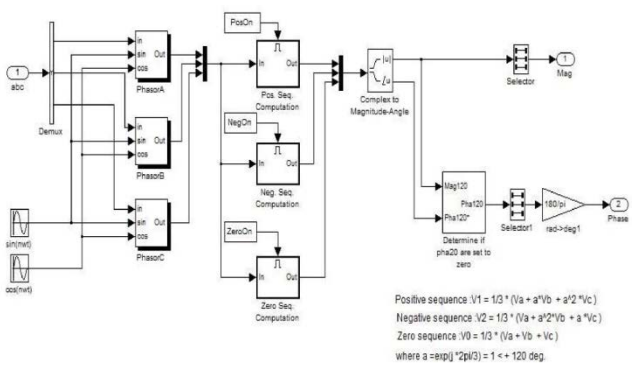

Fig. 8 Sequence Filter Circuit

3.2 Block Descriptions

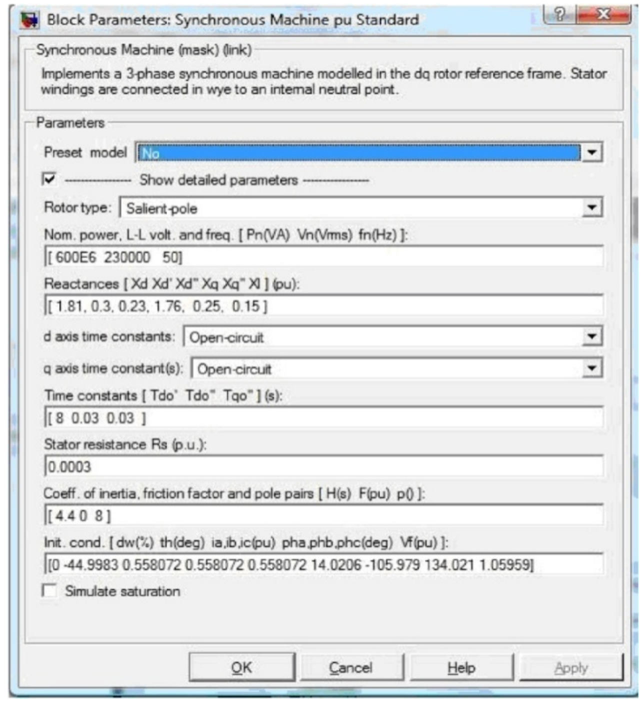

Fig. 9 Synchronous machine pu model

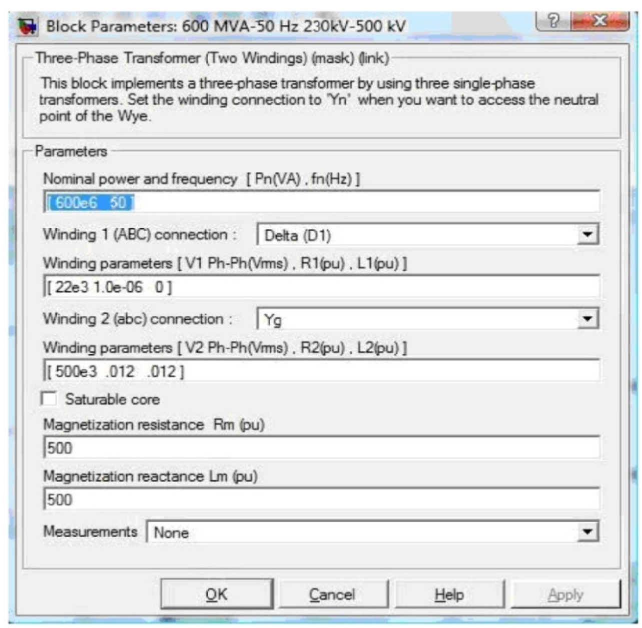

Fig. 10 Transformer

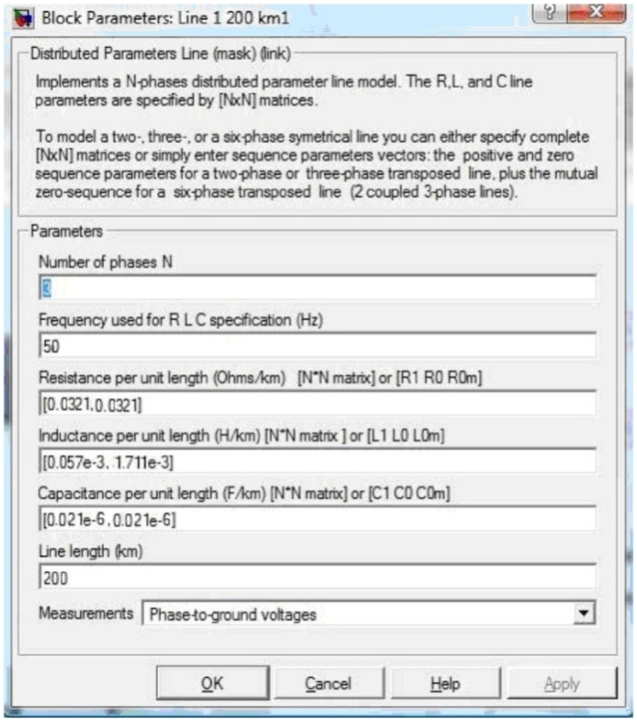

Fig. 11 Transmission Line 1

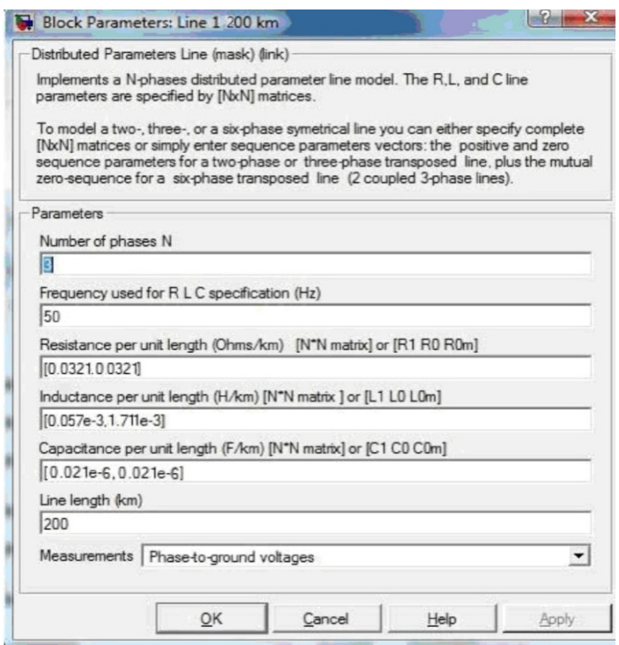

Fig. 12 Transmission Line 2

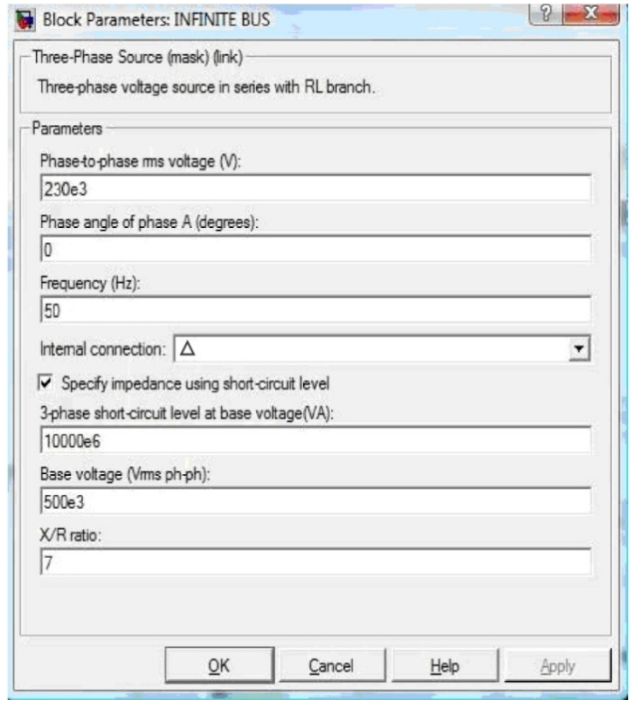

Fig. 13 Infinite Bus

4. Fault Analysis & Detection

4.1 Fault Analysis

The identification of type of fault is done with help of the symmetric components of fault currents at bus 1 and bus 2.

Symmetric components:

By the works of Fortes cue's we know that an unbalanced system of *n* related phasors can be resolved into *n* systems of balanced phasors called the symmetric components of the original phasors. The *n* phasors of each set of component are equal in length, and angle between adjacent phasors are set equal.

According to fortes cue's theorem, three unbalanced phasors of a three phase system can be resolved into three balanced systems of phasors. The balanced sets of components are:

1. Positive sequence component consisting of three phasors of equal in magnitude displaced in angle by 120 degree and having same phase sequence as the original phasors.

2. Negative sequence components consisting of three phasors equal in magnitude displaced in angle by 120 degree and having phase sequence opposite to that of the original phasors.

3. Zero sequence components consisting of three phasors equal in magnitude and with zero phase displacement from each other.

$$I_a = I_{a1} + I_{a2} + I_{a0}$$

$$I_b = I_{b1} + I_{b2} + I_{b0}$$

$$I_c = I_{c1} + I_{c2} + I_{c0}$$

Or in matrix form

$$\begin{bmatrix} I_{a0} \\ I_{a1} \\ I_{a2} \end{bmatrix} = \frac{1}{3} \begin{bmatrix} 1 & 1 & 1 \\ 1 & \alpha & \alpha^2 \\ 1 & \alpha^2 & \alpha \end{bmatrix} \begin{bmatrix} I_a \\ I_b \\ I_c \end{bmatrix}$$

In our model these components have been obtained using the sequence filter circuit. The inputs to above circuit are I_a , I_b and I_c . And the outputs obtained are plots of magnitude and phase of all three components of currents.

4.2 Fault Detection

4.2.1 Single line to ground fault:

In case of single line to ground fault it is observed that zero seq. component is greater in magnitude than negative seq. component at bus1. Whereas at bus2 negative seq.component is greater than zero seq. component. In the figures shown below the colour codes used are:

Zero sequence – green
Positive sequence- yellow
Negative sequence- pink

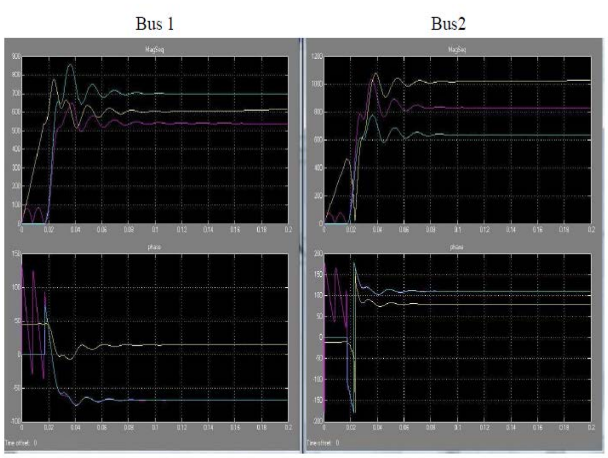

Fig. 14 AG fault

Observation:

Phase of negative seq. component = phase of zero seq. component.

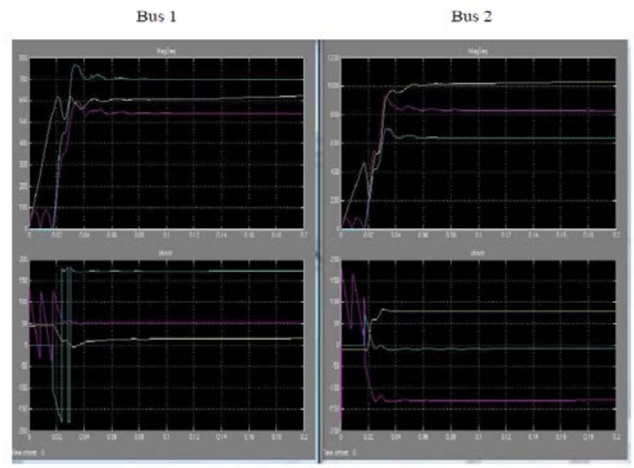

Fig. 15 BG fault

Observation:

Zero sequence component leads negative sequence component by 120^0 at both the buses.

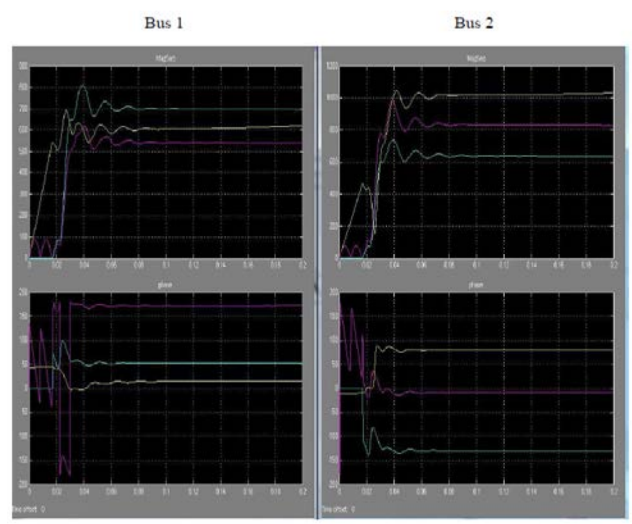

Fig. 16 CG fault

Observation:

Zero sequence component leads negative sequence component by 120^0 at both the buses.

4.2.2. Line to line fault

In case of line to line fault zero sequence component of current is absent at both the busses

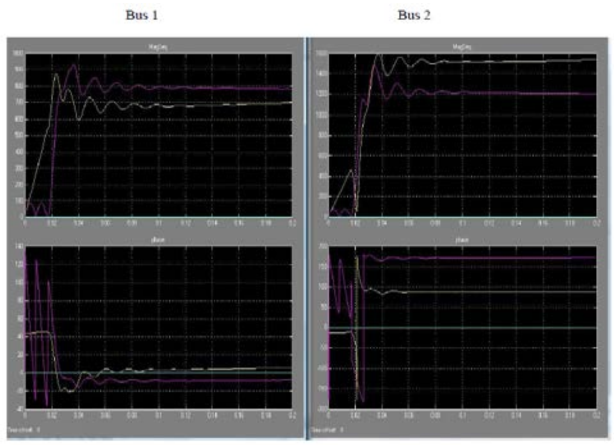

Fig. 17 AB fault

Observation:

At B1 positive seq. component leads negative seq. component.
At B2 positive seq. component lags negative seq. component.
Positive seq. at B1 lags positive seq. at B2 by 90^0.
Negative seq. at B1 lags negative seq. at B2 by 180^0

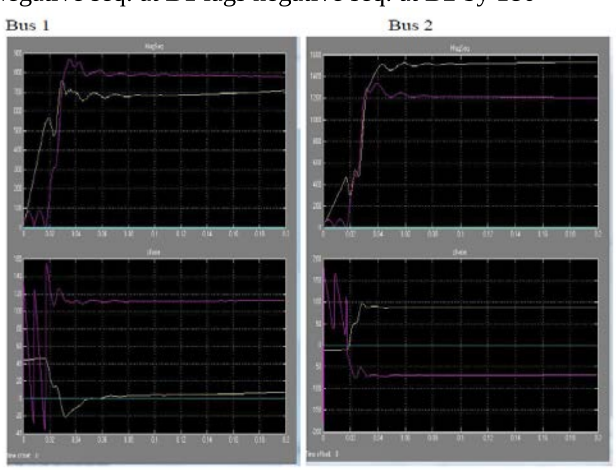

Fig. 18 BC fault

Observation:

At B1 negative seq. leads positive seq. component. At B2 positive seq. leads negative seq. component. Negative seq. at B1 leads negative seq. at B2 by 180^0. Positive seq. at B1 lags positive seq. at B2 by 90^0.

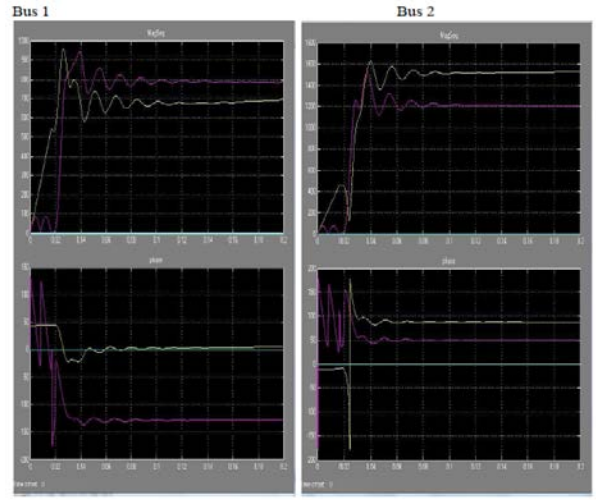

Fig. 19 C-A fault

Observation:

Positive seq. leads negative seq. at both the busses B 1 and B2. Positive seq. at B1 leads positive seq. at B2 by 90^0Negative seq. at B1 lags negative seq. at B2 by 180^0

4.2.3. Three phase fault

Three phase faults, being balanced in nature, have negative sequence current only during transient time.

1. The relative magnitude of Positive and zero sequence component tells whether it is a ground fault.
2. Phase of zero sequence component is always zero.

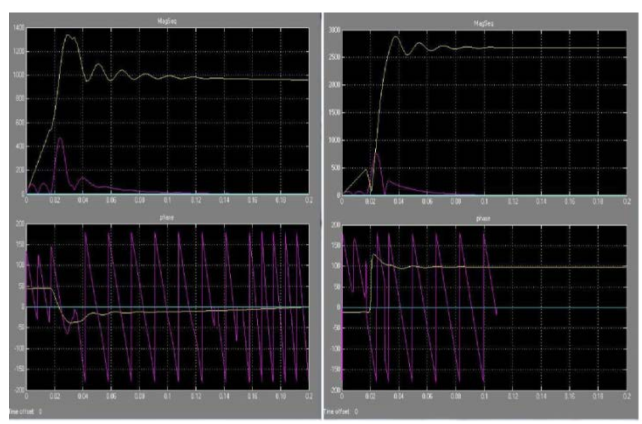

Fig.20 Three Phase fault

Observation:

1. Zero seq. component is not present.

2. Negative seq. component is present only during transient time

5. Fault Location Problem of Fault Resistance in Fault Allocation

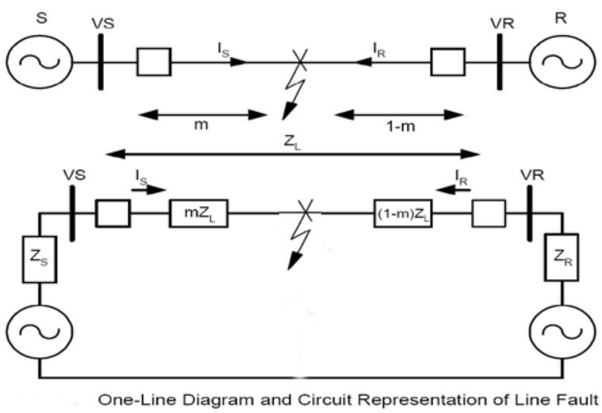

Fig. 21 Circuit. representation of Line Fault

The voltage drop in the above figure 21 from the Sending end of the line is:

$$V_s = I_s m Z_L + I_F R_F \quad (1)$$

The voltage drop in the above figure from the Receiving end of the line is:

$$V_R = I_R(1-m)Z_L + I_F R_F \quad (2)$$

Eliminating $(I_F R_F)$ from equation (7.1) and (7.2)

$$m = (V_S - V_R + I_R * Z_L) \quad (3)$$

Thus, expression holds better accuracy results for three phase shunt faults allocation since independent of fault resistance.

5.1 Types of Shunt Faults

1. L-L-L-G
2. L-L-L
3. L-G
4. L-L
5. L-L-G

The fault location for the proposed scheme has been shown through a series of simulation result from figure 22 to figure 33s.

Simulation Results for L-L-L-G and L-L-L Faults:

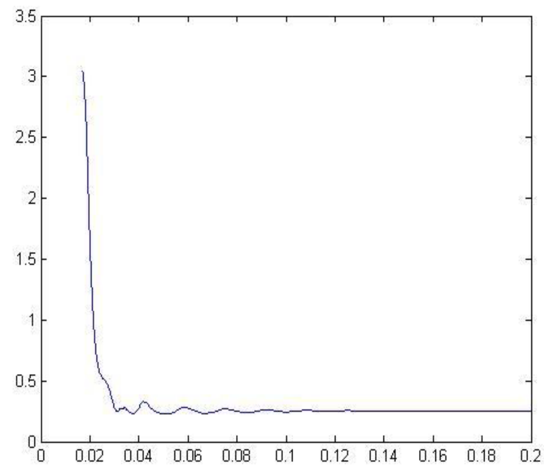

Theoretical m=0.25 Observed (at 0.08 sec) m=0.24 Error -4%

Fig. 22 Plot of ‘m’ vs time for fault resistance 0.001ohm on 280km line, for fault distance of 70 km from B1

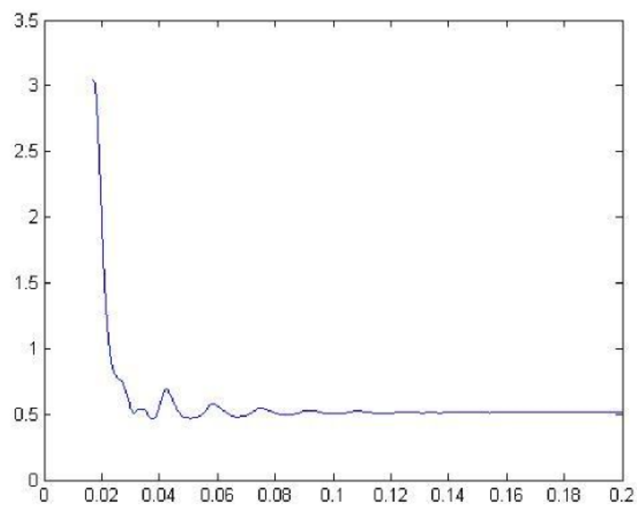

Theoretical m=0.50 Observed (at 0.08 sec) m=0.51 Error 2%

Fig. 23 For fault distance of 140 km from B1

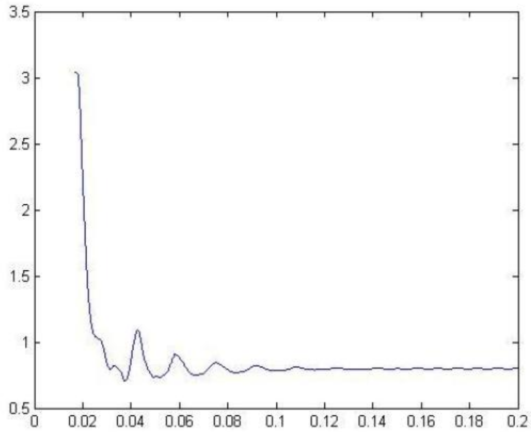

Theoretical m=0.75 Observed (at 0.08 sec) m=0.78 Error 4%

Fig. 24 For fault distance of 210 km from B1

Simulation Results for L-G Faults:

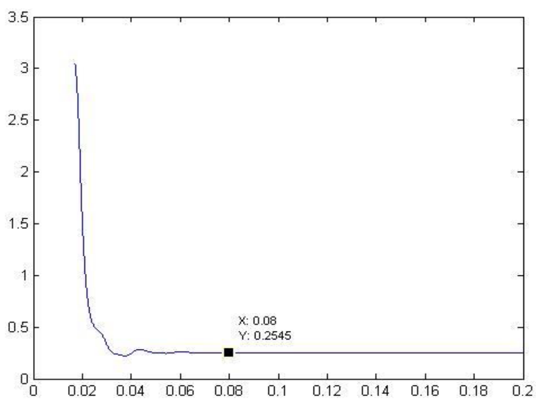

Theoretical m=0.25 Observed (at 0.08 sec) m=0.2545 Error 1.8%

Fig. 25 Plot of ‘m’ vs time for fault resistance 0.001ohm on 280km line, for fault distance of 70 km from B1

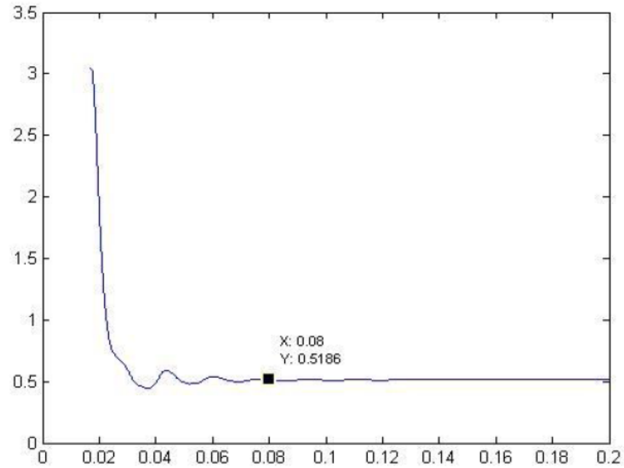

Theoretical m=0.50 Observed (at 0.08 sec) m=0.5186 Error 3.7%

Fig. 26 For fault distance of 140 km from B1

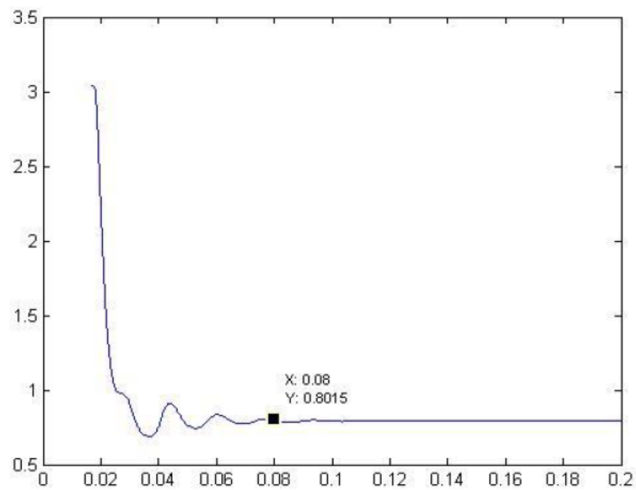

Theoretical m=0.75 Observed (at 0.08 sec) m=0.8015 Error 6%

Fig. 27 For fault distance of 210 km from B1

Simulation Results for Line-Line fault:

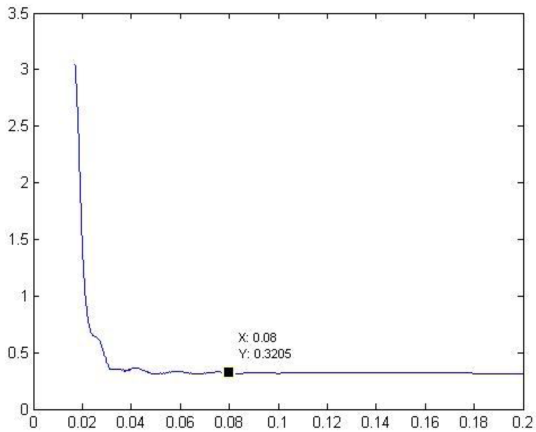

Theoretical m=0.25 Observed (at 0.08 sec) m=0.3205 Error 28%

Fig. 28 Plot of 'm' vs time for fault resistance 0.001ohm on 280km line, for fault distance of 70 km from B1

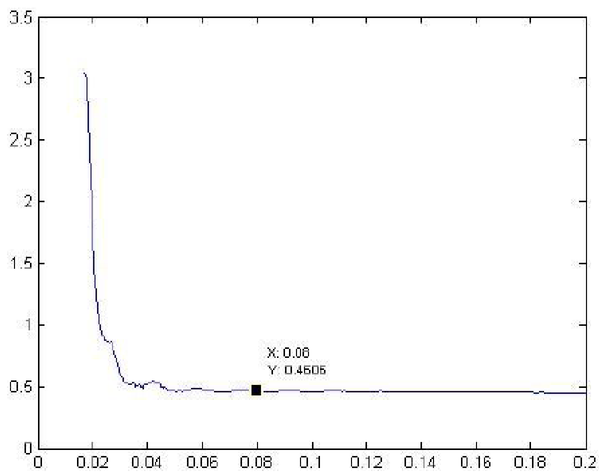

Theoretical m=0.50 Observed (at 0.08 sec) m=0.4606 Error 7.9%

Fig. 29 For fault distance of 140 km from B1

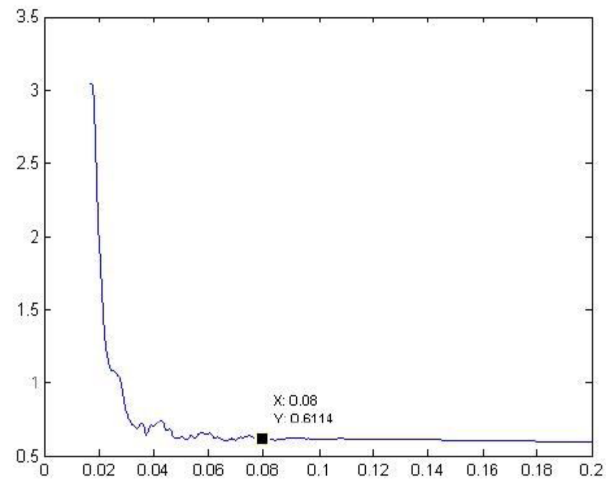

Theoretical m=0.75 Observed (at 0.08 sec) m=0.6114 Error 18.5%

Fig. 30 For fault distance of 210 km from B1

Simulation Results for L-L-G Faults:

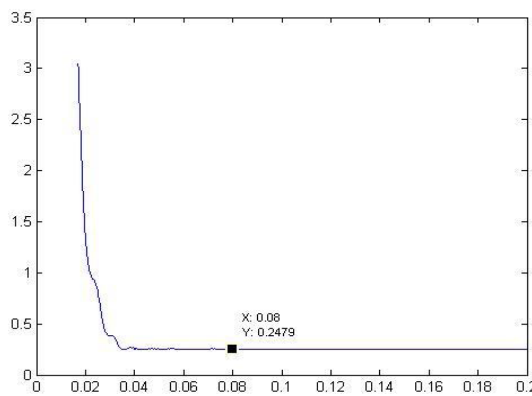

Theoretical m=0.25 Observed (at 0.08 sec) m=0.2479 Error 0.08%

Fig. 31 Plot of 'm' vs time for fault resistance 0.001ohm on 280km line, for fault distance of 70 km from B1

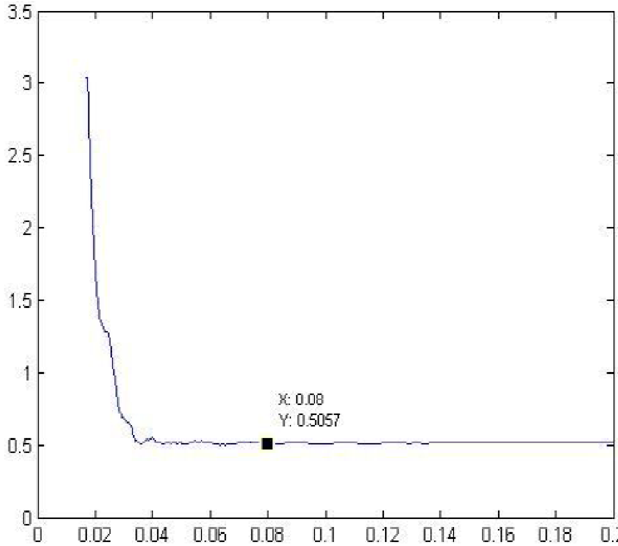

Theoretical m=0.50 Observed (at 0.08 sec) m=0.5057 Error 1.24%

Fig. 32 For fault distance of 140 km from B1

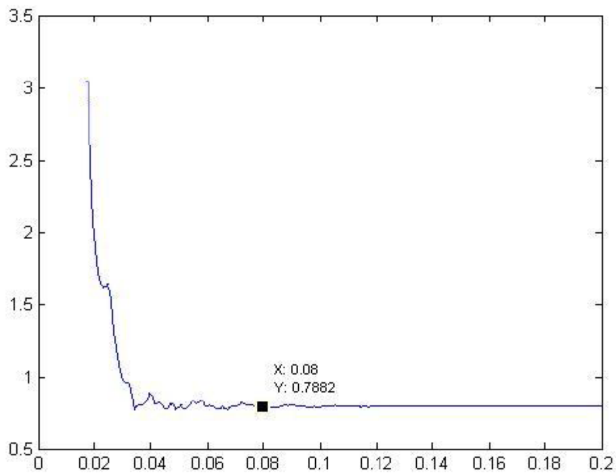

Theoretical m=0.75 Observed (at 0.08 sec) m=0.7882 Error 5%

Fig. 33 For fault distance of 210 km from B1

Graphical comparison of Results

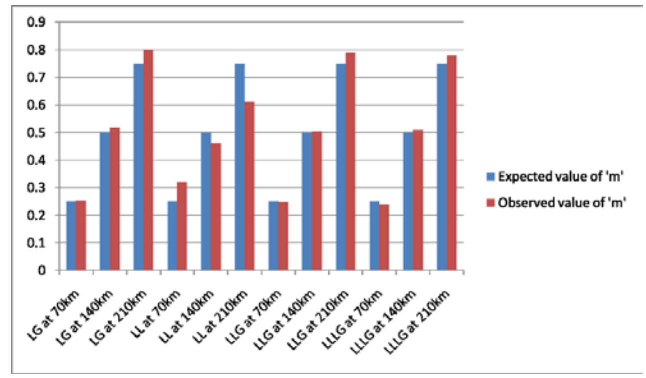

(a)

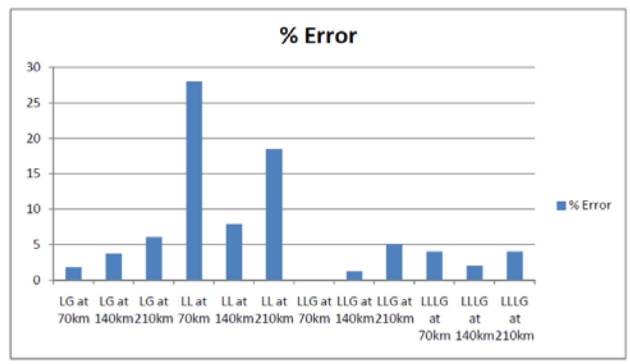

(b)

Fig. 34 (a) Fault resistance of 0.001ohm, (b) Percentage of Error

6. New Approach for Fault Location on Transmission Lines Not Requiring Line Parameters

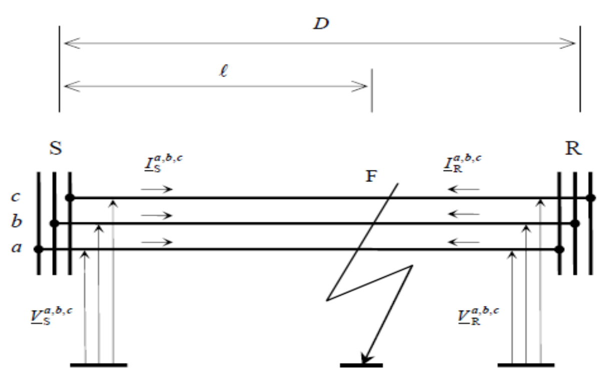

Fig. 35 Three-phase representation of the faulted line

Based on the voltage and current phasors, by using the symmetrical components method, the positive, negative and zero sequence symmetrical components of the voltages and currents can be determined. The new method requires just the positive and negative sequence components, i.e. their equivalent circuits.

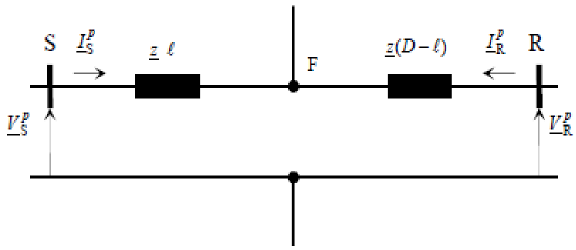

Fig. 36 Equivalent positive sequence circuit of the faulted line

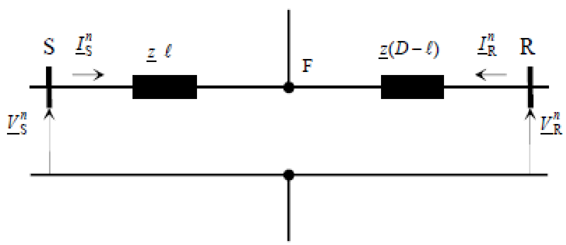

Fig. 37 Equivalent negative sequence circuit of the faulted line

$$V_S{}^P - Z_l I_S{}^P = V_r{}^P - Z_{(D-l)} I_r{}^P \quad (4)$$

$$V_S{}^n - Z_l I_S{}^n = V_r{}^n - Z_{(D-l)} I_r{}^n \quad (5)$$

Where, $V_S{}^{P,n}, V_r{}^{P,n}$ are the positive and negative sequence phase voltages at both line terminals. $I_S{}^{P,n}, I_r{}^{P,n}$ are the positive and negative sequence phase currents at both line terminals. Z_l and $Z_{(D-l)}$ are unknown. They can easily be determined by solving equations (4) and (5). The two solutions are given in following two formulas:

$$Z_l = \frac{\left[(V_S{}^P - V_r{}^P)\, I_r{}^n - (V_S{}^n - V_r{}^n)\, I_r{}^P\right]}{I_S{}^P I_r{}^n - I_S{}^n I_r{}^P} \quad (6)$$

$$Z_{(D-l)} = \frac{\left[(V_S{}^P - V_r{}^P)\, I_S{}^n - (V_S{}^n - V_r{}^n)\, I_S{}^P\right]}{I_S{}^P I_r{}^n - I_S{}^n I_r{}^P} \quad (7)$$

Let us express the distance to the fault, l, as a percentage of the line length, D, through the following formula:

$$l\% = \left(\frac{l}{D}\right) 100 \quad (8)$$

$$l\% = \left[\frac{Z_l}{Z_l + Z_{(D-l)}}\right] \times 100 \quad (9)$$

After including the expressions for Z_l and $Z_{(D-l)}$ in equation (9), the following formula for the distance to the fault can be obtained:

$$l\% = \left[\frac{\left[(V_S{}^P - V_r{}^P)\, I_r{}^n - (V_S{}^n - V_r{}^n)\, I_r{}^P\right]}{(V_S{}^P - V_r{}^P)(I_S{}^n + I_r{}^n) - (V_S{}^n - V_r{}^n)(I_S{}^P + I_r{}^P)}\right] \times 100 \quad (7.10)$$

Obviously, the algorithm does not require the line parameters or information about the line length. It is just based on the processing of synchronously recorded voltage and current samples, determining their 50 Hz phasors, and calculation of the positive and negative sequence voltage and current components.

6.1 Simulation Results for Our Proposed Approach

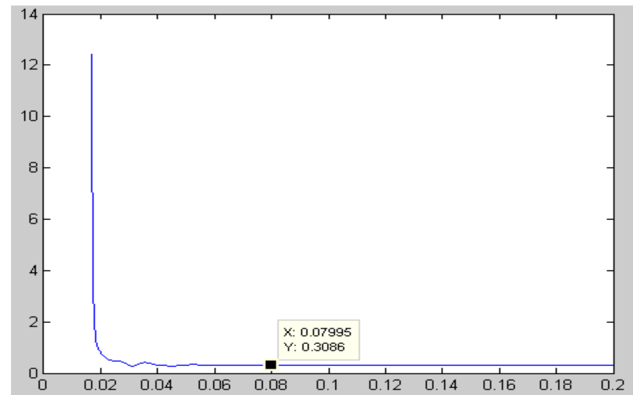

Theoretical m=0.3 Observed (at 0.08 sec) m=0.3086 Error 2.867%

Fig. 38 Plot of 'm' vs time for fault resistance 0.001ohm on 100km line, for fault distance of 30 km from B1

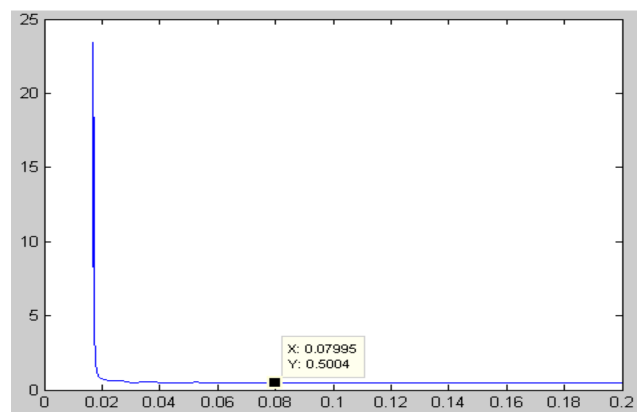

Theoretical m=0.5 Observed (at 0.08 sec) m=0.5004 Error 0.08%

Fig. 39 Plot of 'm' vs time for fault resistance 0.001ohm on 100km line, for fault distance of 50 km from B1

7. Conclusion

As seen from the results, the location of the fault in the given line was estimated with a fair amount of precision and the type of fault in the given system was correctly detected by observing the current waveforms at both the buses for all types of faults in the system. The fault detection and location scheme based on the use of synchrophasors gives more reliable results as compared to the distance protection schemes which are currently being used.

References

[1] A.G. Phadke, "System of Choice-Phasor measurements for real time applications", IEEE Power and Energy Magazine, September/October 2008.
[2] Gabriel Benmouyal, E. O. Schweitzer, A. Guzmán, "Synchronized phasor measurement in protective relays for protection, control, and analysis of electric power systems", presented before 29th annual western protective relay conference spokane, Washington, October 22-24, 2002.
[3] Jonathan Sykes, Kristian Koellner, Dr. William Premerlani, Dr. Bogdan Kasztenny, Mark Adamiak, "synchrophasors: A Primer and practical applications", Presented at the Clemson Power Systems Conference, Clemson University, Clemson, March 13-16, 2007.
[4] Karl Zimmerman and David Costello, "impedance based fault locationexperience", Schweitzer Engineering Laboratories, 2004.
[5] William D. Stevenson Jr., "Elements of power system analysis", McGraw-Hill book Co., 1982.

Mr. Satyabrata Das received the degree in Computer Sc & engineering from Utkal University, in 1996. He received the M.Tech. degree in CSE from ITER, Bhubaneswar. He is a research student of Fakir Mohan University, Balasore in the dept. of I&CT Currently, he is an Asst. Professor at College of Engineering Bhubaneswar, Orissa. His interests are in AI, Soft Computing, Data Mining, DSP, Neural Network.

Dr.Soumya Ranjan Mohanty received the M.Tech. degree in electrical engineering from UCE, Burla. He received the Ph.D. degree in electrical engineering from IIT, Kharagpur. Currently, he is an Asst. professor at Motilal Neheru National Institute of Technology, Allahabad, UP. His research area includes Signal processing application to power system protection, Application of Neural Network for robust classification in transmission line, FACTS etc.

Dr.Sabyasachi Pattnaik received the M.Tech. degree in CSE from IIT, Delhi. He received the Ph.D. degree in Computer Sc from Utkal University. Currently, he is a professor at Fakir Mohan University, Balasore. His research interests include Data Mining, AI and Soft Computing.